Arabian Journal of Chemistry (2020) 13, 2340–2348

King Saud University

Arabian Journal of Chemistry

www.ksu.edu.sa
www.sciencedirect.com

ORIGINAL ARTICLE

Effects of a dianion compound as a surface modifier on the back reaction of photogenerated electrons in TiO_2-based solar cells

Ji Young Kim [a,b], Ki Hong Kim [c], Dae-Hwan Kim [a,*,2], Yoon Soo Han [d,*,1]

[a] *Convergence Research Center for Solar Energy, Daegu Gyeongbuk Institute of Science and Technology (DGIST), Daegu 42988, Republic of Korea*
[b] *Department of Polymer Science and Engineering, Kyungpook National University, Daegu 41566, Republic of Korea*
[c] *Department of Optometry and Vision Science, Daegu Catholic University, Gyeongbuk 38430, Republic of Korea*
[d] *Department of Advanced Materials and Chemical Engineering, Daegu Catholic University, Gyeongbuk 38430, Republic of Korea*

Received 2 February 2018; accepted 26 April 2018
Available online 7 May 2018

KEYWORDS

Dianion compound;
1,2-Ethanedisulfonic acid disodium salt;
Dye-sensitized solar cell;
Back reaction

Abstract The TiO_2 films were modified with a dianion compound, 1,2-ethanedisulfonic acid disodium salt (ESD), to give a negative charge (ethane sulfonate anion) on the TiO_2 surface, i.e., TiO_2-O-SO_2-CH_2-CH_2-SO_3^-), and effects of repulsion between the negative charge and ions (I_3^-) of the electrolyte on the performance of dye-sensitized solar cells (DSSCs) were investigated. The reference device without any modification showed a power conversion efficiency (PCE) of 9.89%, whereas for the device with ESD(20)-TiO_2/FTO, which was prepared by soaking bare TiO_2/FTO in an ESD solution for 20 min, the PCE was increased to 10.97%, due to an increase in both short-circuit current (J_{sc}) and open-circuit voltage(V_{oc}). It was verified from the measurements of electrochemical impedance, open-circuit voltage decay and dark current that the enhancement in the J_{sc} and V_{oc} values was attributed to the reduced back reaction between photoinjected electrons and I_3^- ions, resulting from the presence of the ethane sulfonate anions on the TiO_2 surface.

1. Introduction

Dye-sensitized solar cells (DSSCs) based on a mesoporous TiO_2 photoanode, a Ru-based dye, an I^-/I_3^- electrolyte and a Pt counter electrode are characterized by their reasonable photovoltaic efficiency, low production cost, and non-vacuum fabrication process (Gong et al., 2017; Kakiage et al., 2015), and thus extensive research into the commercialization of them is being conducted. However, DSSCs still cannot compete with Si- or inorganic semiconductor-based solar cells in the market

* Corresponding authors.
E-mail addresses: monolith@dgist.ac.kr (D.-H. Kim), yshancu@cu.ac.kr (Y.S. Han).
[1] Present address: Hayang-ro 13-13, Hayang-eup, Gyeongsan-si, Gyeongbuk 38430, Korea.
[2] Present address: 333 Techno Jungang-daero, Hyeonpung-myeon, Dalseong-gun, Daegu 42988, Korea.
Peer review under responsibility of King Saud University.

ELSEVIER Production and hosting by Elsevier

https://doi.org/10.1016/j.arabjc.2018.04.017
1878-5352

of large-scale energy production due to an insufficient power conversion efficiency (PCE) and reliability. Many investigators have made great efforts to enhance the PCE of DSSCs by improving the constituents' properties. These efforts can largely be classified into four categories of development: new sensitizers (Soliman et al., 2017), anodic materials (Hoa et al., 2014; Dao et al., 2014; Imran et al., 2017), electrolytes (Wu et al., 2015), and electrodes (Dao et al., 2015; Dao and Choi, 2016). Recently, water-based DSSCs have been paied much attention due to their eco-friendly nature and higher reliability. Water-based materials such as poly(3,4-ethylenedioxythio phene) (Mustafa et al., 2017), aqueous NaI/I_2 mixed solution (Gallianoa et al., 2018), cellulose derivatives (Salvador et al., 2014; Bella et al., 2017, 2014) and poly(glycidyl methacrylate) (Imperiyka et al., 2014) have been employed as a counter electrode or an electrolyte to realize non-tocic and reliable solar cells.

The TiO_2 film as a photoelectrode of DSSCs play an important role to adsorb sufficient dye molecules for photoelectron generation and to favorably soak hole-carrying electrolytes, owing to its high surface area, and it is also a good transporter of electrons injected from the photoexcited dyes. Thus, high short-circuit current (J_{sc}) can be achieved from the TiO_2-based cells. However, unlike other solar cells, an electron transporting TiO_2 layer is in direct contact with the hole conductor (electrolyte), inducing the back reaction ($I_3^- + 2e^- \rightarrow 3I^-$) between the photoinjected electrons and ions in the electrolyte. This may cause a loss of approximately 300 mV in the open-circuit voltage (V_{oc}) compared to the theoretical value, which leads to a rapid decrease in the conversion efficiency (Bandaranayake et al., 2004). It has been reported that surface modification of TiO_2 photoelectrodes using semiconducting or insulating metal oxides, metal salts, organic co-adsorbents and acids could control the back reaction (Saxena and Aswal, 2015; Sun et al., 2016). The DSSCs with surface-modified TiO_2 layers have shown an enhancement in PCE attributed to an improved V_{oc}, J_{sc} and/or fill factor (*FF*), resulting from a surface state passivation, formation of energy barrier or formation of surface dipole (O'Regan et al., 2005). And some cases, the PCE improvement by the modifications was due to prevention of direct contact between the TiO_2 layer and the hole conductor (electrolyte).

As far as we know, dianion compounds as a surface modifier had not been applied to DSSCs. Here, we report effects of a dianion compound, 1,2-ethanedisulfonic acid disodium salt (ESD), on the performance of DSSCs. The TiO_2 films were soaked in an aqueous ESD solution to modify their surfaces, and the resulting films (ESD-modified TiO_2) were used as the photoelectrodes of the DSSCs. DSSCs with ESD-modified photoelectrodes were fabricated, and the effects of the surface modification on the photovoltaic performance of the cells were examined.

2. Experimental details

2.1. Materials

Commercial fluorine-doped tin oxide (FTO; sheet resistance ~7 Ω/square) glass (TCO22-7), TiO_2 paste for the photoelectrode (Ti-nanoxide T/SP), TiO_2 paste for the scattering layer (Ti-nanoxide R/SP), N719 dye (Ruthenizer 535-bisTBA), hot-melt adhesive (SX1170-60PF, Surlyn), and iodide-based electrolytes (AN-50) were purchased from Solaronix. The ESD and $TiCl_4$ were purchased from Sigma-Aldrich Co. LLC. Platinum paste (PT-1, Dyesol-Timo) was selected as the source for the Pt counter-electrode. All the chemicals were used without further purification.

2.2. Fabrication of DSSCs

The FTO glasses were cleaned in a detergent solution using sonication for 20 min, and then thoroughly rinsed with deionized water and ethanol. After the ultrasonic cleaning, the FTO glasses were immersed in a 40-mM $TiCl_4$ solution at 70 °C for 30 min, and then washed with water and ethanol. One active TiO_2 layer, which formed on the FTO glass, was prepared via doctor-blade coating with the TiO_2 paste. Additionally, a TiO_2 layer composed of approximately 400-nm-diameter particles was deposited on the active TiO_2 layer and then calcinated at 500 °C for 60 min to produce the scattering layer. Finally, the TiO_2 films were again treated with a 40-mM $TiCl_4$ solution and annealed at 500 °C for 60 min; thus, TiO_2/FTO electrodes with scattering layers were prepared. The electrodes were soaked in an aqueous solution (5×10^{-4} M) of ESD for 0–40 min to deposit anions onto the TiO_2 layers. Next, the resulting electrodes were rinsed with water and ethanol, and then dried at 65 °C for 10 min to produce the modified photoelectrodes (ESD-TiO_2/FTO). The bare TiO_2/FTO and ESD-TiO_2/FTO photoelectrodes were separately immersed into 0.5 mM of N719 dye solution (acetonitrile/*tert*-butyl alcohol, v/v = 1) for 24 h to obtain working electrodes.

To prepare the counter-electrode, two holes were formed in the FTO glass with a drill, and then cleaned with the method described above. A Pt layer was formed on the FTO glass via the doctor-blade method using Pt paste, followed by a calcination process at 400 °C for 30 min. The thermally treated platinum counter-electrodes were placed on the photoelectrodes and sealed with a 60-μm-thick sealing material. The electrolyte was introduced into the cells through one of the two small holes drilled on the counter-electrodes to produce DSSCs with a 25 mm^2 active area.

2.3. Measurements

X-ray photoelectron spectroscopy (XPS) was performed using VG Multilab ESCA 2000 (ThermoVG Scientific) with Mg Kα radiation. The C 1s photoelectron peak (binding energy of 284.6 eV) was used as an energy reference. Fourier transform infrared (FT-IR) spectra were recorded on a FT/IR 4100 spectrometer (Jasco) equipped with an attenuated total reflectance (ATR, PRO450-S, Jasco). Field emission scanning electron microscopy (FE-SEM; S-4800, Hitachi High-Technology) was used to study the morphology of the photoelectrodes. The photocurrent–voltage measurement was performed using a CompactStat (Ivium Technologies B.V.) potentiostat and a PEC-L01 solar simulator system equipped with a 150 W xenon arc lamp (Peccell Technologies, Inc.). The light intensity was adjusted to 1 sun (100 mW/cm^2) with a silicon photodiode (model PEC-SI01, Peccell Technologies, Inc.). The UV–vis absorption spectra were obtained using a SINCO NEOSYS-2000 spectrophotometer. Both the electrochemical impedance spectroscopic (EIS) analysis and the open-circuit voltage decay

(OCVD) measurements were performed using an electrochemical analyzer (CompactStat, Ivium Technologies B.V.). The active areas of the dye-adsorbed TiO_2 films were estimated using a digital microscope camera (OLYMPUS SZ61) with image analysis software.

3. Results and discussion

3.1. Adsorption of anions on TiO_2 surface

The bare TiO_2/FTO was soaked in an aqueous ESD solution for 10–40 min to prepare ESD(10, 20, 30, and 40)-TiO_2/FTO, where "(10)" means that the dipping time was 10 min. To confirm the incorporation of anions ($-SO_3^-$), an XPS measurement was conducted using the ESD(20)-TiO_2/FTO electrode. However, the peaks attributed to sulfur were not detected. This could have occurred because the concentration of sulfonate group on the TiO_2 surface is below the detection limit of the XPS instrument. When the dipping time was prolonged for 24 hr, sulfur peaks appeared as shown in Fig. 1. The peaks detected at 167.89 and 169.08 eV corresponds to the $2p_{3/2}$ and $2p_{1/2}$ binding energies in S, respectively, indicating that, by the simple dipping in each solution, sulfate ions were adsorbed on the TiO_2 surface. To further confirm the incorporation of the sulfonate groups, ATR-FTIR spectra were recorded for the ESD-modified TiO_2 film. However, absorption peaks measured from the ESD(20)-TiO_2 film, which was dipped into the ESD solution for 20 min, were almost similar to those of bare TiO_2 film, probably due to the small amount of ESD in ESD(20)-TiO_2. Thus, we provide the ATR-FTIR spectrum for 60-min-treated TiO_2 [ESD(60)-TiO_2] film. Fig. 2 shows the IR spectra of bare TiO_2, ESD(20)-TiO_2 and ESD(60)-TiO_2 films. In contrast to bare TiO_2 and ESD(20)-TiO_2, the stronger absorption band at 1092 cm^{-1}, assignable to the stretching vibrations of S═O═S bonds, appeared in the spectrum of the ESD(60)-TiO_2 film, strongly supporting the presence of sulfonate groups (Albishri et al., 2017; Lokman et al., 2016). Several research groups have also reported that sulfonate groups can be adsorbed onto TiO_2 surface by the soaking process (Khazraji et al., 1999; Zhang and Cole, 2015). It appears the ESD adsorbed on TiO_2 surface will be maintained for a certain operation time of the cells since it is not dissolved in the electrolyte and acetronitrile.

In order to investigate the morphological changes by the ESD modification, SEM images were obtained. However, a comparison of the images revealed no noticeable change in morphology as shown in Fig. 3. We believe that the ESD adsorbed with very low concentration does not affect the surface morphology. From the SEM images, it can be seen that the working electrode is consisted of about 7-μm-thick photoanode and 3-μm-thick scattering layer.

3.2. Performance variations of DSSCs with bare and ESD-modified TiO_2 photoelectrodes

We expected that the one end (anion) of ESD would be adsorbed on TiO_2 surface, and its other anion would be exposed to the electrolyte, i.e., TiO_2-O-SO_2-CH_2-CH_2-SO_3^-, as shown in Fig. 4. The exposed anions (-SO_3^-) would repulse I_3^- in the electrolyte, and thus reduce the back reaction between the photoinjected electrons and I_3^-. This could lead to an improvement in the performance of the DSSCs.

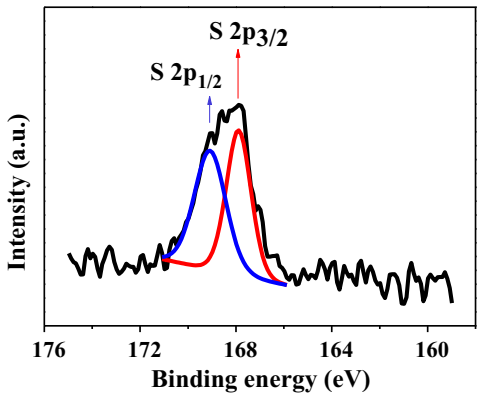

Fig. 1 XPS spectra for S 2p measured using ESD(20)-TiO_2/FTO.

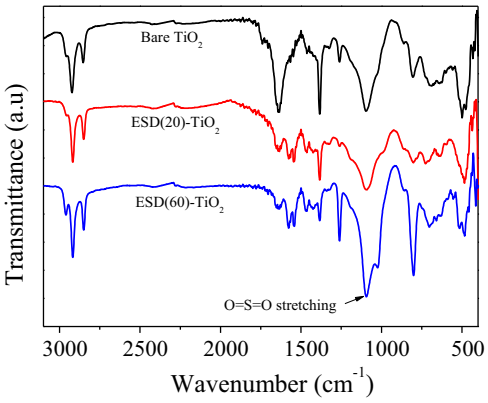

Fig. 2 ATR-FTIR spectra of bare, ESD(20)- and ESD(60)-TiO_2/FTO.

To confirm the incorporation effects of anions, DSSCs with ESD-modified TiO_2/FTO electrodes were fabricated, and their photovoltaic properties (Table. 1) was compared to a reference device with bare TiO_2/FTO, i.e., without any surface treatment. Fig. 5 shows performance variations of the DSSCs as a function of the soaking time. The J_{sc} and V_{oc} values of the DSSCs with ESD-TiO_2/FTO were increased for all the soaking time, compared to those of the reference cell, and the maximum values were recorded when the dipping time in the ESD solution was 20 min. There were no meaningful changes in *FF* values in the devices. Overall, PCE values were increased by the incorporation of ESD on the surface of TiO_2 electrodes. Because the highest PCE value was observed when the TiO_2/FTO electrode was dipped in the ESD solution for 20 min, we focused on this device with ESD(20)-TiO_2/FTO to investigate the origin of the efficiency enhancement.

The photovoltaic properties of the DSSCs with bare TiO_2/FTO and ESD(20)-TiO_2/FTO are compared in Fig. 6 and Table 1. The device with ESD(20)-TiO_2/FTO showd a PCE of 10.97%. When compared with that (9.89%) of the reference cell with pristine TiO_2/FTO, about 11% enhancement in PCE was achieved, which was attributed to an increase in J_{sc} and V_{oc}.

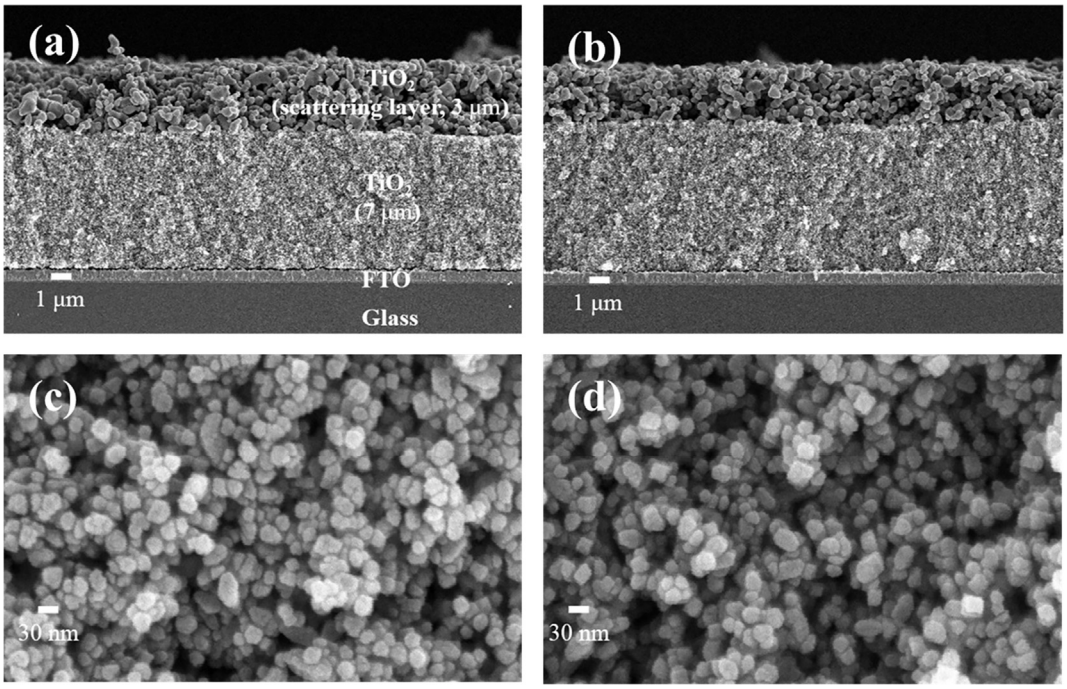

Fig. 3 Cross-sectional SEM images of (a) bare TiO_2/FTO and (b) ESD(20)-TiO_2/FTO photoelectrodes; (c) and (d) are also cross-sectional SEM images of TiO_2 layer in bare TiO_2/FTO and ESD(20)-TiO_2/FTO, respectively.

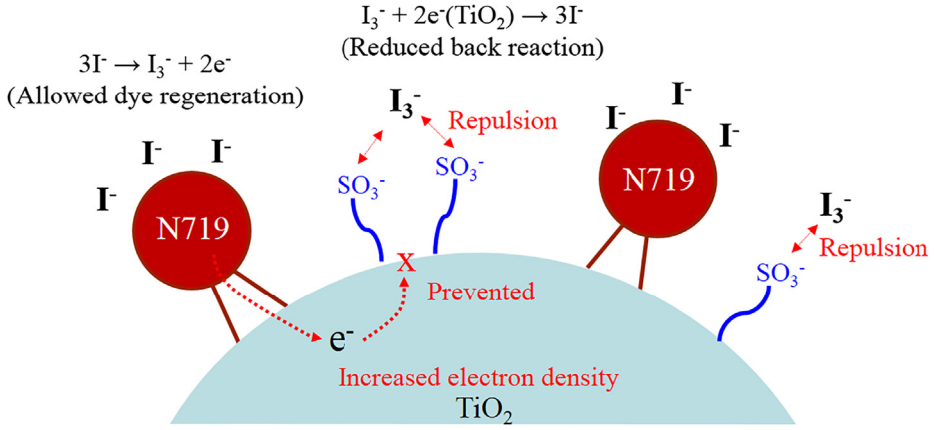

Fig. 4 Schematic illustration of the reduced back reaction by the repulsion between sulfonate anions and I_3^-.

Table 1 Photovoltaic properties of the DSSCs with bare TiO_2/FTO and ESD-modified TiO_2/FTO electrodes.

Applied electrodes	J_{sc} (mA/cm^2)	V_{oc} (mV)	*FF* (%)	η (%)
Bare TiO_2/FTO	20.36	0.698	69.59	9.89
ESD(10)-TiO_2/FTO	21.45	0.704	69.44	10.49
ESD(20)-TiO_2/FTO	22.28	0.716	68.79	10.97
ESD(30)-TiO_2/FTO	21.63	0.708	69.37	10.62
ESD(40)-TiO_2/FTO	21.35	0.704	69.87	10.50

3.3. Influences of the ESD modification on J_{sc}

By the ESD modification, J_{sc} increased from 20.36 for bare TiO_2/FTO to 22.28 mA/cm^2 for ESD(20)-TiO_2/FTO (Table 1). The J_{sc} value is generally influenced by four efficiency factors, as shown in Eqs. (1) and (2), i.e., the light harvesting (LHE), electron injection (η_{inj}), dye regeneration (η_{reg}), and electron collection (η_{coll}) efficiencies of the injected electrons to the

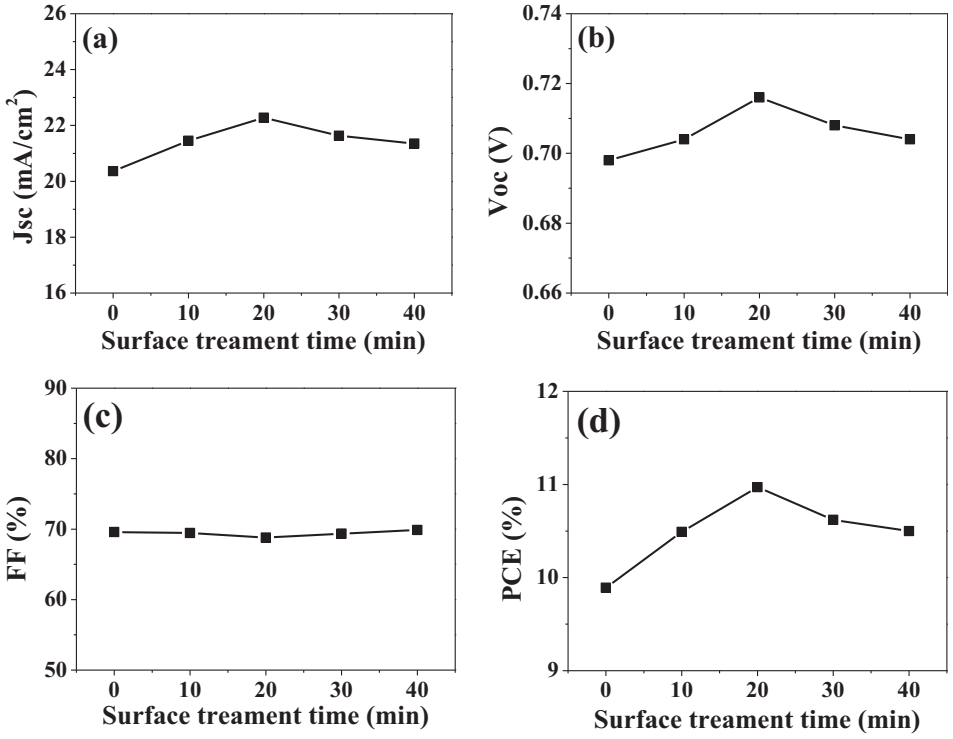

Fig. 5 Variations of performance with soaking time in the ESD solution; (a) J_{sc}, (b) V_{oc}, (c) *FF*, and (d) *PCE* of the DSSCs, measured under AM 1.5 irradiation.

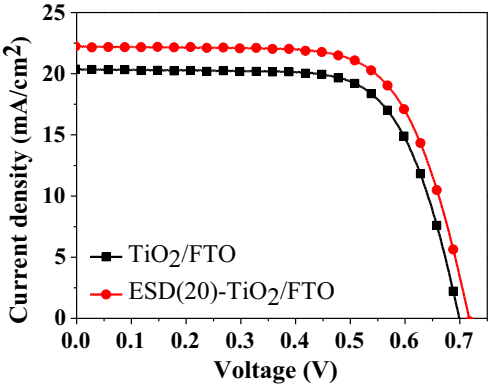

Fig. 6 *J–V* characteristics of the DSSCs with bare TiO_2/FTO and ESD(20)-TiO_2/FTO electrodes.

transparent electrode, where e is the elementary charge and $\Phi_{\mathrm{ph,AM1.5G}}$ is the photon flux in AM 1.5 G, 100 mW/cm^2 (Hagfeldtt et al., 2010; Arkan et al., 2016).

$$J_{sc} = \int \mathrm{IPCE}(\lambda) e \Phi_{ph,AM1.5G}(\lambda) d\lambda \quad (1)$$

$$\mathrm{IPCE}(\lambda) = \mathrm{LHE}(\lambda)\eta_{\mathrm{inj}}(\lambda)\eta_{\mathrm{reg}}\eta_{\mathrm{coll}}(\lambda) \quad (2)$$

The LHE is related to the light absorbance (A) of the adsorbed dyes, i.e., LHE = $1–10^{-A}$ (Hagfeldtt et al., 2010; Arkan et al., 2016). Thus, to investigate the effects of the LHE on the J_{sc} enhancement, the amount of adsorbed dyes was first measured using the Beer-Lambert equation ($A = \varepsilon bc$), where the molar extinction coefficient (ε) for N719 in the basic aqueous solution is 1.25×10^4 M^{-1} cm^{-1} at 500 nm, and b is the width of the quartz cell (1 cm in this study) (Alarcón et al. (2007); Lee et al., 2012; Kim and Han, 2014). The average dye loading amounts, measured using 10 cells, for the bare TiO_2/FTO and the ESD(20)-TiO_2/FTO electrodes were 6.21×10^{-5} and 6.33×10^{-5} mol/cm^3, respectively. The amount of adsorbed dye molecules on the ESD(20)-TiO_2/FTO electrode was almost similar to that on the bare TiO_2/FTO film, indicating that the ESD modification of TiO_2 surface did not affect the LHE, and thus the J_{sc} value.

The η_{inj} value could be varied by the shift of conduction band edge (CBE). To confirm the CBE shift, we measured UV–visible absorption and valence band spectra of bare TiO_2/FTO and ESD(20)-TiO_2/FTO (Fig. 7). The absorption edge of ESD(20)-TiO_2/FTO was at 370.8 nm, which could be assigned to a band gap of 3.36 eV. Bare TiO_2/FTO exhibited an absorption edge of 367.4 nm corresponding to the band gap of 3.38 eV. The position of the valence band edge (VBE) of ESD(20)-TiO_2/FTO could be seen at about 3.83 eV_{NHE} (NHE = Normal Hydrogen Electrode), which was the same as that of bare TiO_2/FTO. The energies of the VBE of ESD (20)-TiO_2/FTO and bare TiO_2/FTO were estimated to be −8.33 eV_{AVS}, because the relationship between E_{NHE} and E_{AVS} (AVS = Absolute Vacuum Scale) is $E_{AVS} = E_{NHE} - E^e$, where E^e (about 4.50 eV) is the energy of free electrons in the hydrogen scale (Sun et al., 2014). Based on the band gap energies, the energies of the CBE of ESD(20)-TiO_2/FTO and bare TiO_2/FTO were determined to be −4.97 and −4.95 eV_{AVS}, respectively. Overall, the energies of CBE in both ESD(20)-TiO_2/FTO and bare TiO_2/FTO was almost the same. It is probably because amount of ESD adsorbed on TiO_2 surface was very small, and anions (TiO_2-O-SO_2-CH_2-CH_2-SO_3^-)

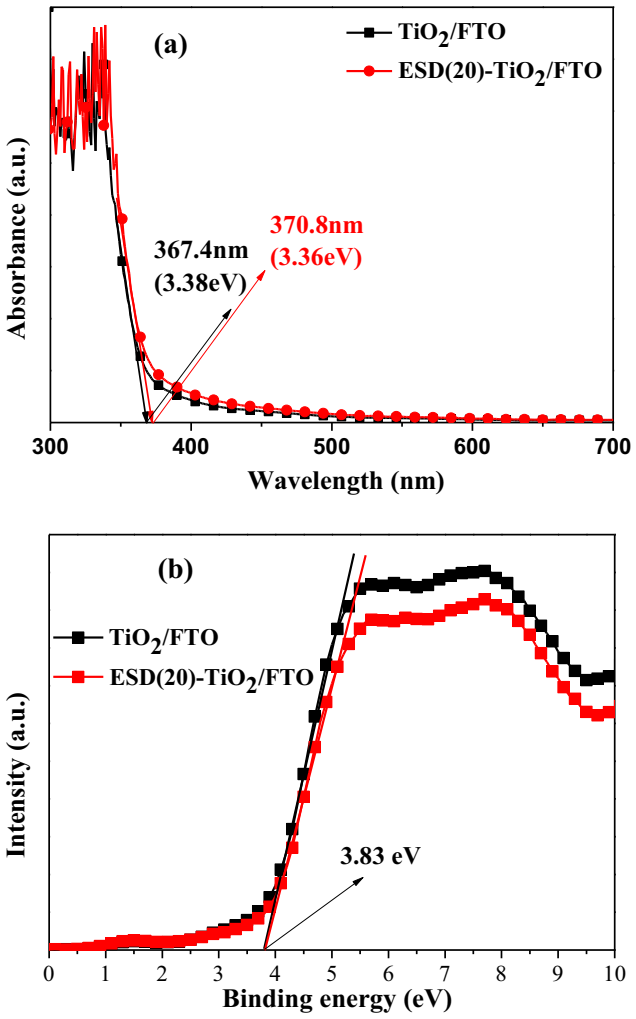

Fig. 7 UV–visible absorbance (a) and UPS valence band (b) spectra for bare and ESD(20)-TiO_2/FTO.

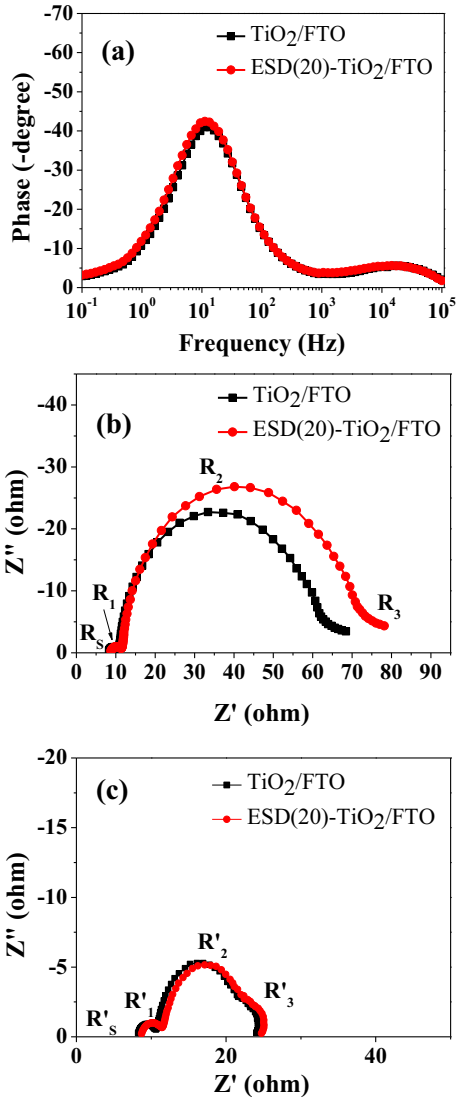

Fig. 8 EIS spectra of the DSSCs with bare TiO_2/FTO and ESD (20)-TiO_2/FTO. (a) Bode and (b) Nyquist plots measured at −0.7 V in the dark and (c) Nyquist plots measured under illumination.

were far from the TiO_2 surface. Thus the ESD modification of TiO_2 surface did not affect the J_{sc} value.

The value of η_{coll} depends on the ratio of the charge transport through TiO_2 to the back reaction of photoinjected electrons, i.e., $\eta_{coll} = K_t/(K_t + K_b) = 1/(1 + K_b/K_t)$, where K_b and K_t are the rate constants for the back reaction and the charge transport, respectively (Kim et al., 2015; Park et al., 2012; Yu et al., 2017). This equation shows that η_{coll} can be improved by decreasing K_b and by increasing K_t. The K_b value is related to the lifetime of electrons injected from the dyes, i.e., a prolonged electron lifetime indicates a decrease in K_b.

EIS has been widely used for investigating the kinetics and energetics of charge transport and interfacial charge recombination in DSSCs (Sarker et al., 2017; Kim et al., 2012; Mohamed et al., 2016; Wang and Hu, 2015; Zhao et al., 2012; Tian et al., 2010; Park et al., 2011; Xu et al., 2014). Fig. 8(a) shows the Bode phase plots of the EIS spectra for the DSSCs with the corresponding photoelectrodes measured at −0.7 V in the dark. Using the peak frequency (f_{max}) of 13.38 and 11.24 Hz obtained from the EIS Bode phase plots of the DSSCs with bare TiO_2/FTO and ESD(20)-TiO_2/FTO, respectively, the electron lifetime (τ_n) was estimated from the equation: $\tau_n = 1/2\pi f_{max}$ (Kim et al., 2012; Mohamed et al., 2016). The electron lifetime was calculated to be 11.89 and 14.16 ms for the DSSCs with bare TiO_2/FTO and ESD(20)-TiO_2/FTO electrodes, respectively. A prolonged lifetime (approximately 19% increase) of the electrons injected from the dyes was obtained for the device with ESD(20)-TiO_2/FTO compared to that of the reference cell. Fig. 8(b) shows the Nyquist plots of the EIS spectra for the DSSCs measured at −0.7 V in the dark. Electrochemical parameters are attributed to the serial resistance, which is determined by the sheet resistance of FTO and electrical contact between TiO_2/FTO interface (R_s), the redox reaction at the platinum counter-electrode (R_1), the electron transfer at the TiO_2/dye/electrolyte interface (R_2), and the carrier transport by ions within the electrolytes (R_3) (Mohamed et al., 2016; Wang and Hu, 2015). It was noted that the ESD modification increased the impedance component in R_2. The larger semicircle of R_2 measured in the dark indicates that the back reaction at the TiO_2/dye/electrolyte interface is

weaker (Zhao et al., 2012; Tian et al., 2010). Thus, the prolonged electron lifetime (Bode plots) and the retardation of the back reaction (Nyquist plots) indicate that K_b was reduced by the ESD modification. Fig. 8(c) shows the Nyquist plots of the EIS spectra for the DSSCs in an open-circuit condition under illumination by simulated AM 1.5 solar light (100 mA/cm^2). When the EIS measurements are conducted in an open-circuit condition, a smaller semicircle in the medium-frequency region indicates a more efficient charge transfer process at the TiO_2/dye/electrolyte interface (Kim et al., 2012; Park et al., 2011; Xu et al., 2014). However, the impedance components of R_2' in the DSSCs with bare TiO_2/FTO and ESD(20)-TiO_2/FTO were measured to be approximately 10.9 Ω. This result demonstrates that the K_t values in both DSSCs are almost similar, i.e., a similar charge transfer process occurs at the TiO_2/dye/electrolyte interface. As a result, we can conclude that the ESD modification induced a decreased K_b, while the K_t value was almost maintained. A decrease in K_b, caused by delayed back reaction, led to an increase of the electron lifetime, which can contribute to the enhancement of η_{coll}. This is likely to be because the ethane sulfonate anions on the TiO_2 surface push out the I_3^- in the electrolyte.

To further confirm the prolonged electron lifetimes in the DSSC with ESD(20)-TiO_2/FTO, the OCVD characteristics of the devices were measured. Typically used to study recombination kinetics in DSSCs, OCVD is a technique that monitors the subsequent decay of the photovoltage (V_{oc}) after stopping the illumination in a steady state (Park et al., 2011; Xu et al., 2014; Lamberti et al., 2013). The cells are maintained under constant illumination in an open-circuit condition until they reach a steady voltage value. At this point, the light is suddenly switched off, and the photovoltage is measured as a function of time. Because some photogenerated electrons cannot be collected by the electrode under the open-circuit condition, they react with I_3^- in the electrolyte at an approximately constant rate, thereby reducing the photovoltage. Consequently, the photovoltage decay rate is directly related to the electron lifetime because excess electrons are removed through the back reaction. Specifically, the recombination rate of photoelectrons is proportional to the photovoltage decay rate. To estimate the electron lifetime (τ) of the devices, the corresponding curves for τ versus voltage (Fig. 9(b)) can be obtained from the OCVD curves (Fig. 9(a)) by using Eq. (3), where k_B is the Boltzmann constant, T is the absolute temperature, e is the electron charge, and dV_{oc}/dt is the first derivative of the open-circuit voltage transient (Hagfeldtt et al., 2010; Park et al., 2011; Xu et al., 2014; Lamberti et al., 2013):

$$\tau = -\frac{k_B T}{e}\left(\frac{dVoc}{dt}\right)^{-1} \quad (3)$$

The electron lifetimes in the DSSC with ESD(20)-TiO_2/FTO were longer than those in the reference device with bare TiO_2/FTO film, as shown in Fig. 9(b). This indicates that the back reaction in the former DSSC was delayed, thereby inducing a prolonged electron lifetime, which also improved η_{coll} in that device.

The dark current values can be used to estimate the back reaction in DSSCs (Chen et al., 2001; Diamant et al., 2003). Fig. 10 shows the dark currents of DSSCs with bare TiO_2/FTO and ESD(20)-TiO_2/FTO as a function of the applied potential. Throughout the measured potential range, the dark current values of the device with ESD(20)-TiO_2/FTO were lower than those of the reference device, which indicated that the back reaction between injected electrons and I_3^- ions was retarded by the incorporation of ESD with a terminal anion. The observation of the delayed back reaction (or the prolonged electron lifetime) was consistent with the results of the EIS and OCVD measurements.

Overall, it is believed that the enhancement in the J_{sc} value of the DSSC with ESD(20)-TiO_2/FTO was mainly attributed to the improvement in η_{coll}. It is because the exposed anions (SO_3^-) repulse I_3^- of the electrolyte, and thus reduce the back reaction between the photoinjected electrons and I_3^-.

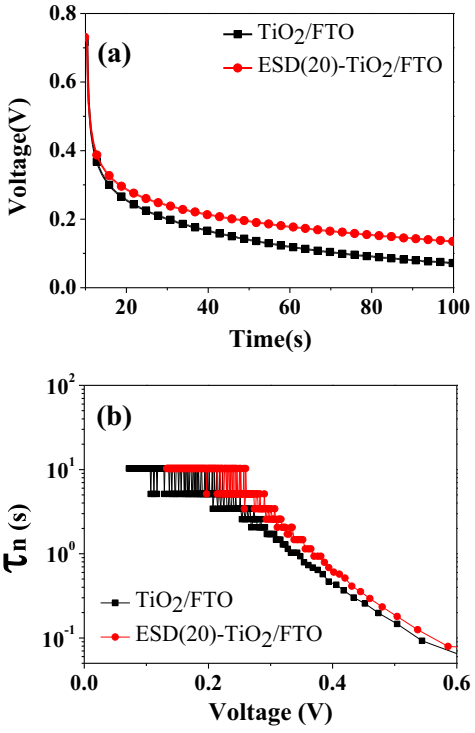

Fig. 9 Curves of OCVD (a) and electron lifetime versus V_{oc} (b) for the DSSCs with bare TiO_2/FTO and ESD(20)-TiO_2/FTO.

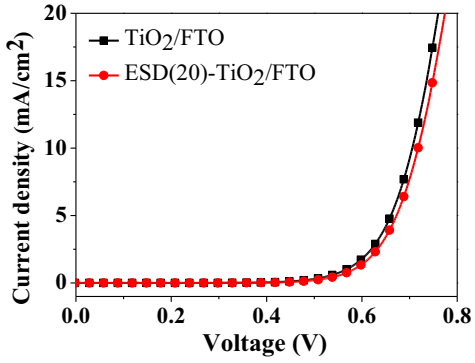

Fig. 10 Dark current–voltage characteristics of DSSCs with bare TiO_2/FTO and ESD(20)-TiO_2/FTO.

3.4. Influences of the ESD modification on V_{oc}

The V_{oc} value (0.716 V) of the DSSC with the ESD(20)-TiO_2/FTO electrode also increased compared with the reference device (0.698 V), which contributed to the increase of the cell efficiency. Under constant illumination, the V_{oc} value of DSSCs corresponds to the increase of the quasi-Fermi level (E_{Fn}) of the semiconductor with respect to the dark value (E_{F0}), and thus it can be expressed as Eq. (4) (Peng et al., 2015; Zaban et al., 2003):

$$V_{oc} = \frac{E_{Fn} - E_{F0}}{e} = \frac{k_B T}{e} ln\left(\frac{n}{n_0}\right) \quad (4)$$

where k_BT is the thermal energy (4.11×10^{-21} J at 25 °C). For more details, k_B and T are the Boltzmann constant and the absolute temperature, respectively. e is the positive elementary charge (1.602×10^{-19} C), n_0 is the concentration in the dark, and n is the free electron density in the TiO_2 photoelectrode under illumination.

Eq. (4) suggests that V_{oc} and n are directly correlated, and n is affected by both the electron injection from the light-absorbed dyes to the conduction bands of TiO_2 and the back reaction between photoinjected electrons and ions (I_3^-) in the electrolyte. Accordingly, higher electron injection and lesser back reaction are required to increase n, which can improve the V_{oc} value. In our case, it is considered that the back reaction is predominant to influence the V_{oc} value, probably because the electron injection efficiency is not altered by the ESD modification due to the similar amounts of adsorbed dyes. As presented above, EIS, OCVD and dark current measurements revealed that the ESD modification (i.e., the incorporation of ethane sulfonate anions) increased the lifetime of the photoinjected electrons, and therefore lowered the back reaction. This indicates that the n value in Eq. (4) increased. Consequentially, the ESD modification led to an increased n, thereby inducing an enhancement in V_{oc} based on Eq. (4).

4. Conclusions

To reduce the back reaction between photoinjected electrons and I_3^- in the electrolyte, a negative charge (ethane sulfonate anions) was formed on TiO_2 surface by soaking bare TiO_2/FTO film to an ESD solution. The modified TiO_2 layer was applied to the photoelectrodes of the DSSCs. The DSSC with ESD(20)-TiO_2/FTO showed an increase in J_{sc} and V_{oc}, resulting in a PCE of 10.97% (J_{sc} = 22.28 mA/cm^2, V_{oc} = 716 mV and FF = 68.79%), compared to that of the reference device with bare TiO_2/FTO (PCE = 9.89%, J_{sc} = 20.36 mA/cm^2, V_{oc} = 698 mV and FF = 68.59%). The incorporation of the ethane sulfonate anions on TiO_2 surface led to about 11% improvement in PCE, because the anions could repulse I_3^-, and thereby reduce the back reaction. It is worth mentioning that the anion incorporation on TiO_2 surface is a good strategy to increase performance of DSSCs by a retardation of the back reaction.

Acknowledgments

This work was supported by the DGIST R&D Program of the Ministry of Science, ICT, and Future Planning of Korea (18-ET-01). This research was also supported by the Basic Science Research Program of the National Research Foundation of Korea (NRF), funded by the Ministry of Science and ICT (NRF-2016R1A2B1015037).

References

Alarcón, H., Hedlund, M., Johansson, E.M.J., Rensmo, H., Hagfeldt, A., Boschloo, G., 2007. Modification of nanostructured TiO_2 electrodes by electrochemical Al^{3+} insertion: effects on dye-sensitized solar cell performance. J. Phys. Chem. C 111, 13267–13274.

Albishri, H.M., Marwani, H.M., Batterjee, M.G., Soliman, E.M., 2017. Eriochrome Blue Black modified activated carbon as solid phase extractor for removal of Pb(II) ions from water samples. Arabian J. Chem. 10, S1955–S1962.

Arkan, F., Izadyar, M., Nakhaeipour, A., 2016. The role of the electronic structure and solvent in the dye-sensitized solar cells based on Zn-porphyrins: theoretical study. Energy 114, 559–567.

Bandaranayake, K.M.P., Senevirathna, M.K.I., Weligamuwa, P.M.G. M.P., Tennakone, K., 2004. Dye-sensitized solar cells made from nanocrystalline TiO_2 films coated with outer layers of different oxide materials. Coord. Chem. Rev. 248, 1277–1281.

Bella, F., Chiappone, A., Nair, J.R., Meligrana, G., Gerbaldi, C., 2014. Effect of different green cellulosic matrices on the performance of polymeric dye-sensitized solar cells. Chem. Eng. Trans. 41, 211–216.

Bella, F., Galliano, S., Falco, M., Viscardi, G., Barolo, C., Grätzel, M., Gerbaldi, C., 2017. Approaching truly sustainable solar cells by the use of water and cellulose derivatives. Green Chem. 19, 1043–1051.

Chen, S.G., Chappel, S., Diamant, Y., Zaban, A., 2001. Preparation of Nb_2O_5 Coated TiO_2 nanoporous electrodes and their application in dye-sensitized solar cells. Chem. Mater. 13, 4629–4634.

Dao, V.-D., Choi, H.-S., 2016. Highly-efficient plasmon-enhanced dye-sensitized solar cells created by means of dry plasma reduction. Nanomaterials. 6, 70(1–9).

Dao, V.-D., Larina, L.L., Choi, H.-S., 2014. Plasma reduction of nanostructured TiO_2 electrode to improve photovoltaic efficiency of dye-sensitized solar cells. J. Electrochem. Soc. 161, H896–H902.

Dao, V.-D., Larina, L.L., Choi, H.-S., 2015. Suppression of charge recombination in dye-sensitized solar cells using the plasma treatment of fluorine-doped tin oxide substrates. J. Electrochem. Soc. 162, H903–H909.

Diamant, Y., Chen, S.G., Melamed, O., Zaban, A., 2003. Core–shell nanoporous electrode for dye sensitized solar cells: the effect of the $SrTiO_3$ shell on the electronic properties of the TiO_2 core. J. Phys. Chem. B 107, 1977–1981.

Gallianoa, S., Bella, F., Piana, G., Giacona, G., Viscardi, G., Gerbaldi, C., Grätzel, M., Barolo, C., 2018. Finely tuning electrolytes and photoanodes in aqueous solar cells by experimental design. Sol. Energy 163, 251–255.

Gong, J., Sumathy, K., Qiao, Q., Zhou, Z., 2017. Review on dye-sensitized solar cells (DSSCs): advanced techniques and research trends. Renew. Sustain. Energy Rev. 68, 234–246.

Hagfeldtt, A., Boschloo, G., Sun, L., Kloo, L., Petterson, H., 2010. Dye-sensitized solar cells. Chem. Rev. 110, 6595–6663.

Hoa, N.T.Q., Dao, V.-D., Choi, H.-S., 2014. A facial one-pot synthesis of hierarchical TiO_2 nanourchins for highly efficient dye-sensitized solar cells. J. Electrochem. Soc. 161, H627–H632.

Imperiyka, M., Ahmad, A., Hanifah, S.A., Bella, F., 2014. A UV-prepared linear polymer electrolyte membrane for dye-sensitized solar cells. Physica B 450, 151–154.

Imran, M., Haider, S., Ahmad, K., Mahmood, A., Al-masry, W.A., 2017. Fabrication and characterization of zinc oxide nanofibers for renewable energy applications. Arabian J. Chem. 10, S1067–S1072.

Kakiage, K., Aoyama, Y., Yano, T., Oya, K., Fujisawa, J., Hanaya, M., 2015. Highly-efficient dye-sensitized solar cells with collabora-

tive sensitization by silyl-anchor and carboxy-anchor dyes. Chem. Commun. 51, 15894–15897.
Khazraji, A.C., Hotchandani, S., Das, S., Kamat, P.V., 1999. Controlling Dye (Merocyanine-540) aggregation on nanostructured TiO_2 films. An organized assembly approach for enhancing the efficiency of photosensitization. J. Phys. Chem. B 103, 4693–4700.
Kim, J.T., Han, Y.S., 2014. Effects of surface-modified photoelectrode on the power conversion efficiency of dye-sensitized solar cell. Met. Mater. Int. 20, 571–575.
Kim, J.T., Lee, S.H., Han, Y.S., 2015. Enhanced power conversion efficiency of dye-sensitized solar cellswith Li_2SiO_3-modified photoelectrode. Appl. Surf. Sci. 333, 134–140.
Kim, K.S., Song, H., Nam, S.H., Kim, S.-M., Jeong, H., Kim, W.B., Jung, G.Y., 2012. Fabrication of an efficient light-scattering functionalized photoanode using periodically aligned ZnO hemisphere crystals for dye-sensitized solar cells. Adv. Mater. 24, 792–798.
Lamberti, A., Sacco, A., Bianco, S., Manfredi, D., Armandi, M., Quaglio, M., Tresso, E., Pirri, C.F., 2013. An easy approach for the fabrication of TiO_2 nanotube-based transparent photoanodes for dye-sensitized solar cells. Sol. Energy 95, 90–98.
Lee, K.E., Gomez, M.A., Charbonneau, C., Demopoulos, G.P., 2012. Enhanced surface hydroxylation of nanocrystalline anatase films improves photocurrent output and electron lifetime in dye sensitized solar cell photoelectrodes. Electrochim. Acta 67, 208–215.
Lokman, I.M., Rashid, U., Taufiq-Yap, Y.H., 2016. Meso- and macroporous sulfonated starch solid acid catalyst for esterification of palm fatty acid distillate. Arabian J. Chem. 9, 179–189.
Mohamed, I.M.A., Dao, V.-D., Barakat, N.A.M., Yasin, A.S., Yousef, A., Choi, H.-S., 2016. Efficiency enhancement of dye-sensitized solar cells by use of ZrO_2-doped TiO_2 nanofibers photoanode. J. Colloid Interf. Sci. 476, 9–19.
Mustafa, M.N., Shafie, S., Zainal, Z., Sulaiman, Y., 2017. Poly(3,4-ethylenedioxythiophene) doped with various carbon-based materials as counter electrodes for dye sensitized solar cells. Mater. Des. 136, 249–257.
O'Regan, B.C., Scully, S., Mayer, A.C., Palomares, E., Durrant, J., 2005. The effect of Al_2O_3 barrier layers in TiO_2/Dye/CuSCN photovoltaic cells explored by recombination and DOS characterization using transient photovoltage measurements. J. Phys. Chem. B 109, 4616–4623.
Park, J.-H., Kim, J.-Y., Kim, J.-H., Choi, C.-J., Kim, H., Sung, Y.-E., Ahn, K.-S., 2011. Enhanced efficiency of dye-sensitized solar cells through $TiCl_4$-treated, nanoporous-layer-covered TiO_2 nanotube arrays. J. Power Sources 196, 8904–8908.
Park, J.T., Roh, D.K., Chi, W.S., Patel, R., Kim, J.H., 2012. Fabrication of double layer photoelectrodes using hierarchical TiO_2 nanospheres for dye-sensitized solar cells. J. Ind. Eng. Chem. 18, 449–455.
Peng, T., Shi, W., Wu, S., Ying, Z., Ri, J.H., 2015. Sea urchin-like TiO_2 microspheres as scattering layer of nanosized TiO_2 film-based dye-sensitized solar cell with enhanced conversion efficiency. Mater. Chem. Phys. 164, 238–245.
Salvador, G.P., Pugliese, D., Bella, F., Chiappone, A., Sacco, A., Bianco, S., Quaglio, M., 2014. New insights in long-term photovoltaic performance characterization of cellulose-based gel electrolytes for stable dye-sensitized solar cells. Electrochim. Acta 146, 44–51.
Sarker, S., Seo, H.W., Seo, D.-W., Kim, D.M., 2017. Electrochemical impedance spectroscopy of dye-sensitized solar cells with different electrode geometry. J. Ind. Eng. Chem. 45, 56–60.
Saxena, V., Aswal, D. K., 2015. Surface modifications of photoanodes in dye sensitized solar cells: enhanced light harvesting and reduced recombination. Semicond. Sci. Technol. 30, 064005-1–23.
Soliman, A.A., Amin, M.A., El-Sherif, A.A., Sahin, C., Varlikli, C., 2017. Synthesis, characterization and molecular modeling of new ruthenium (II) complexes with nitrogen and nitrogen/oxygen donor ligands. Arabian J. Chem. 10, 389–397.
Sun, L., Yue, Q., Hia, C.-J., Jin, Z., Fan, W., 2014. Enhanced visible-light photocatalytic activity of g-C_3N_4/Zn_2GeO_4 heterojunctions with effective interfaces based on band match. Nanoscale 6, 2649–2659.
Sun, Q., Li, Y., Dou, J., Wei, M., 2016. Improving the efficiency of dye-sensitized solar cells by photoanode surface modifications. Sci. China. Mater. 59, 867–883.
Tian, H., Hu, L., Zhang, C., Liu, W., Huang, Y., Mo, L., Guo, L., Sheng, J., Dai, S., 2010. Retarded charge recombination in dye-sensitized nitrogen-doped TiO_2 solar cells. J. Phys. Chem. C 114, 1627–1632.
Wang, H., Hu, Y., 2015. Electro-catalytic role of insulator/conductor interface in MgO/PEDOT composite electrodes for dye-sensitized solar cells. Sci. China Chem. 58, 101–106.
Wu, J., Lan, Z., Lin, J., Huang, M., Huang, Y., Fan, L., Luo, G., 2015. Electrolytes in dye-sensitized solar cells. Chem. Rev. 115, 2136–2173.
Xu, J., Fan, K., Shi, W., Li, K., Peng, T., 2014. Application of ZnO micro-flowers as scattering layer for ZnO-based dye-sensitized solar cells with enhanced conversion efficiency. Sol. Energy 101, 150–159.
Yu, M., Qu, Y., Pan, K., Wang, G., Li, Y., 2017. Enhanced photoelectric conversion efficiency of dye-sensitized solar cells by the synergetic effect of $NaYF_4$:Er^{3+}/Yb^{3+} and g-C_3N_4. Sci. China Mater 60, 228–238.
Zaban, A., Greenshtein, M., Bisquert, J., 2003. Determination of the electron lifetime in nanocrystalline dye solar cells by open-circuit voltage decay measurements. ChemPhysChem. 4, 859–864.
Zhang, L., Cole, J.M., 2015. Anchoring groups for dye-sensitized solar cells. ACS Appl. Mater. Interfaces 7, 3427–3455.
Zhao, J., Sun, B., Qiu, L., Caocen, H., Li, Q., Chena, X., Yan, F., 2012. Efficient light-scattering functionalized TiO_2 photoanodes modified with cyanobiphenyl-based benzimidazole for dye-sensitized solar cells with additive-free electrolytes. J. Mater. Chem. 22, 18380–18386.